Bull Volcanol (2014) 76:817
DOI 10.1007/s00445-014-0817-7

RESEARCH ARTICLE

Late Quaternary history of the Vakinankaratra volcanic field (central Madagascar): insights from luminescence dating of phreatomagmatic eruption deposits

Daniel Rufer · Frank Preusser · Guido Schreurs · Edwin Gnos · Alfons Berger

Received: 22 November 2012 / Accepted: 12 March 2014 / Published online: 5 April 2014
© Springer-Verlag Berlin Heidelberg 2014

Abstract The Quaternary Vakinankaratra volcanic field in the central Madagascar highlands consists of scoria cones, lava flows, tuff rings, and maars. These volcanic landforms are the result of processes triggered by intracontinental rifting and overlie Precambrian basement or Neogene volcanic rocks. Infrared-stimulated luminescence (IRSL) dating was applied to 13 samples taken from phreatomagmatic eruption deposits in the Antsirabe–Betafo region with the aim of constraining the chronology of the volcanic activity. Establishing such a chronology is important for evaluating volcanic hazards in this densely populated area. Stratigraphic correlations of eruption deposits and IRSL ages suggest at least five phreatomagmatic eruption events in Late Pleistocene times. In the Lake Andraikiba region, two such eruption layers can be clearly distinguished. The older one yields ages between 109±15 and 90±11 ka and is possibly related to an eruption at the Amboniloha volcanic complex to the north. The younger one gives ages between 58±4 and 47±7 ka and is clearly related to the phreatomagmatic eruption that formed Lake Andraikiba. IRSL ages of a similar eruption deposit directly overlying basement laterite in the vicinity of the Fizinana and Ampasamihaiky volcanic complexes yield coherent ages of 68±7 and 65±8 ka. These ages provide the upper age limit for the subsequently developed Iavoko, Antsifotra, and Fizinana scoria cones and their associated lava flows. Two phreatomagmatic deposits, identified near Lake Tritrivakely, yield the youngest IRSL ages in the region, with respective ages of 32±3 and 19±2 ka. The reported K-feldspar IRSL ages are the first recorded numerical ages of phreatomagmatic eruption deposits in Madagascar, and our results confirm the huge potential of this dating approach for reconstructing the volcanic activity of Late Pleistocene to Holocene volcanic provinces.

Keywords Luminescence dating · Quaternary volcanism · Geochronology · Madagascar · Vakinankaratra · Phreatomagmatic deposits · Ankaratra

Editorial responsibility: G. Giordano

D. Rufer · G. Schreurs (✉) · A. Berger
Institute of Geological Sciences, Baltzerstrasse 1 + 3, University of Bern, 3012 Bern, Switzerland
e-mail: schreurs@geo.unibe.ch

F. Preusser
Department of Physical Geography and Quaternary Geology, Stockholm University, 10691 Stockholm, Sweden

E. Gnos
Muséum d'histoire naturelle de Genève, route de Malagnou 1, CP 6434, 1211 Genève 6, Switzerland

Introduction

In the central highlands of Madagascar, volcanic rocks of the Itasy and Ankaratra volcanic fields overlie Precambrian basement rocks (Fig. 1). These two fields form part of a Late Cenozoic magmatic cycle that is mainly found in central and northern Madagascar, with a few small outliers in the southwest (Besairie 1964; Rasamimanana et al. 1998; Bardintzeff et al. 2010). Late Cenozoic magmatism is associated with intracontinental rifting that is affecting Madagascar since mid-Miocene times (Bertil and Regnoult 1998; Laville et al. 1998; Piqué et al. 1999). Rifting in Madagascar has been related to the East African Rift system (Mougenot et al. 1986; Laville et al. 1998), with deformation becoming more distributed and diffuse towards the south (Kusky et al. 2007, 2010).

Located southwest of Antananarivo, the Ankaratra volcanic field (Fig. 1) contains both Tertiary and Quaternary volcanic rocks, with the latter mostly restricted to its southwestern margin (Mottet 1980a, b). We use the term "Vakinankaratra volcanic field" for the Quaternary volcanic

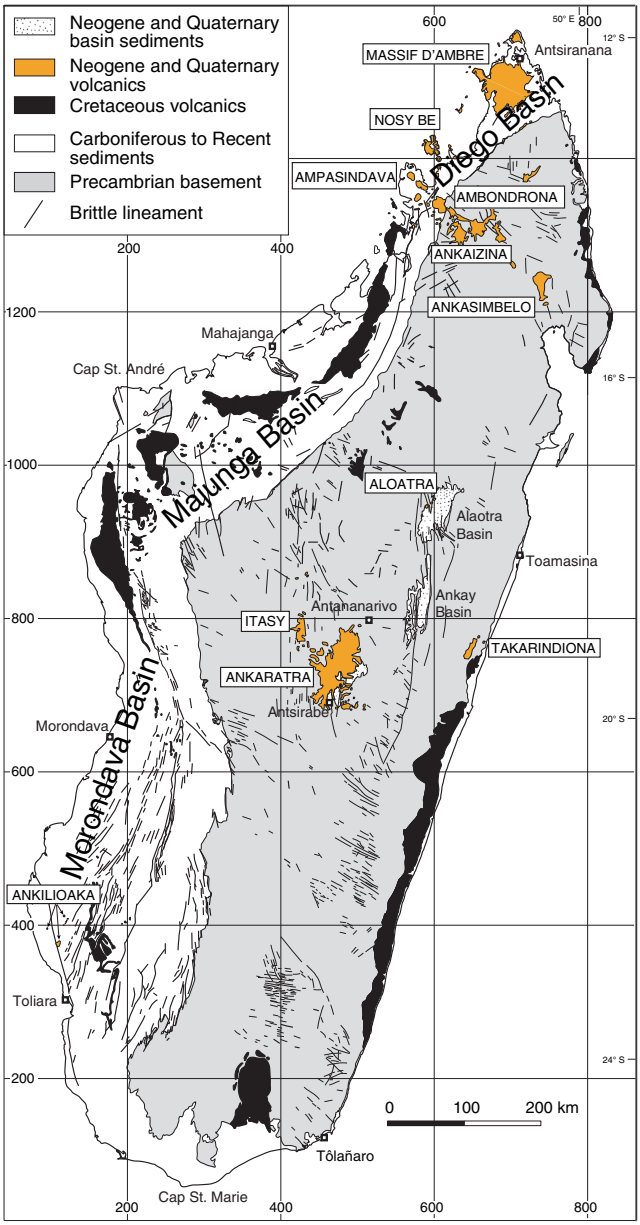

Fig. 1 Simplified geological map of Madagascar with location of Cretaceous and Neogene and Quaternary volcanic fields (after Besairie 1964). *Grid* shows Laborde coordinates

rocks in the southwestern part of the Ankaratra field, in the area between Antsirabe and Betafo (Fig. 2). The limited direct or indirect age data available suggest that volcanic activity in the Vakinankaratra field occurred during the Late Pleistocene and possibly Holocene (Gasse and Van Campo 1998).

Obtaining accurate ages on the young volcanic rocks of the Vakinankaratra field is important not only for geomorphologic and climate studies, but also for volcanic hazard assessment studies in this densely populated area. However, methods for directly dating volcanic rocks of Late Quaternary age are scarce, not always straightforward, and possess some inherent pitfalls. Dating methods using radioactive decay systems require closed system behavior, a suitable parent isotope-rich constituent, and sufficient accumulation of radiogenic daughter isotopes for accurate and precise measurements (e.g., Faure 1986). Our initial attempts to date the volcanic rocks of the Vakinankaratra field using the $^{40}Ar/^{39}Ar$ method failed due to the young age of the material, overall low potassium concentrations in whole rock samples, and a lack of measurable sanidine. Furthermore, the abundance of xenocrysts together with an open system behavior of uranium in phlogopite prevented uranium-thorium dating, whereas the lack of organic material associated with the volcanic deposits impeded the application of radiocarbon dating. Here, we present an overview of phreatomagmatic activity in the Vakinankaratra volcanic field and present the first numerical age data of such eruption deposits in Madagascar using luminescence methods.

General geological setting

Madagascar is a continental island with a central highland plateau at a mean elevation of c. 1,200 m. The eastern two-thirds of the island, including the central highland plateau, consist almost exclusively of high-grade metamorphic Precambrian basement, whereas the remaining one third to the west comprises Late Paleozoic to Quaternary sedimentary and volcanic cover rocks.

A major magmatic episode in Late Cenozoic times resulted in large volcanic fields mainly in central and northern Madagascar (e.g., Ankaratra, Itasy, Takarindoha, or Takarindiona, see Tucker and Moine (2012) for discussion on toponymy; Massif d'Ambre) and local dyke swarms (e.g., near Ankilioaka, SW Madagascar; Bardintzeff et al. 2010). This Late Cenozoic magmatism is temporally and spatially associated with intracontinental rifting that is considered an extension of the Somalian-African diffusive plate boundary (Kusky et al. 2010). Since mid-Miocene times, the entire southwestern edge of the Indian Ocean, including the Davie Ridge in the Mozambique Channel, the Comoros Archipelago, and Madagascar has come under an overall E-W extensional regime (Bertil and Regnoult 1998). This resulted in extensional reactivation of the Davie Ridge (Grimison and Chen 1988) and the formation of major N-S trending rift graben basins in the central highlands of Madagascar, such as the c. 250 km long Plio-Pleistocene Alaotra-Ankay graben system (Fig. 1; Laville et al. 1998; Piqué et al. 1999; Kusky et al. 2010), and the half-grabens near Antsirabe (Mottet 1980a, b). Scattered, but frequent seismicity characterizes the island of Madagascar with magnitudes up to M=5.8 (Bertil and Regnoult 1998) and earthquake focal mechanisms indicating mainly normal faulting (Grimison and Chen 1988). Seismicity is particularly concentrated in the region of the Ankaratra and Itasy volcanic fields and in the immediate vicinity of the Ankay-Alaotra graben system (Bertil and Regnoult 1998).

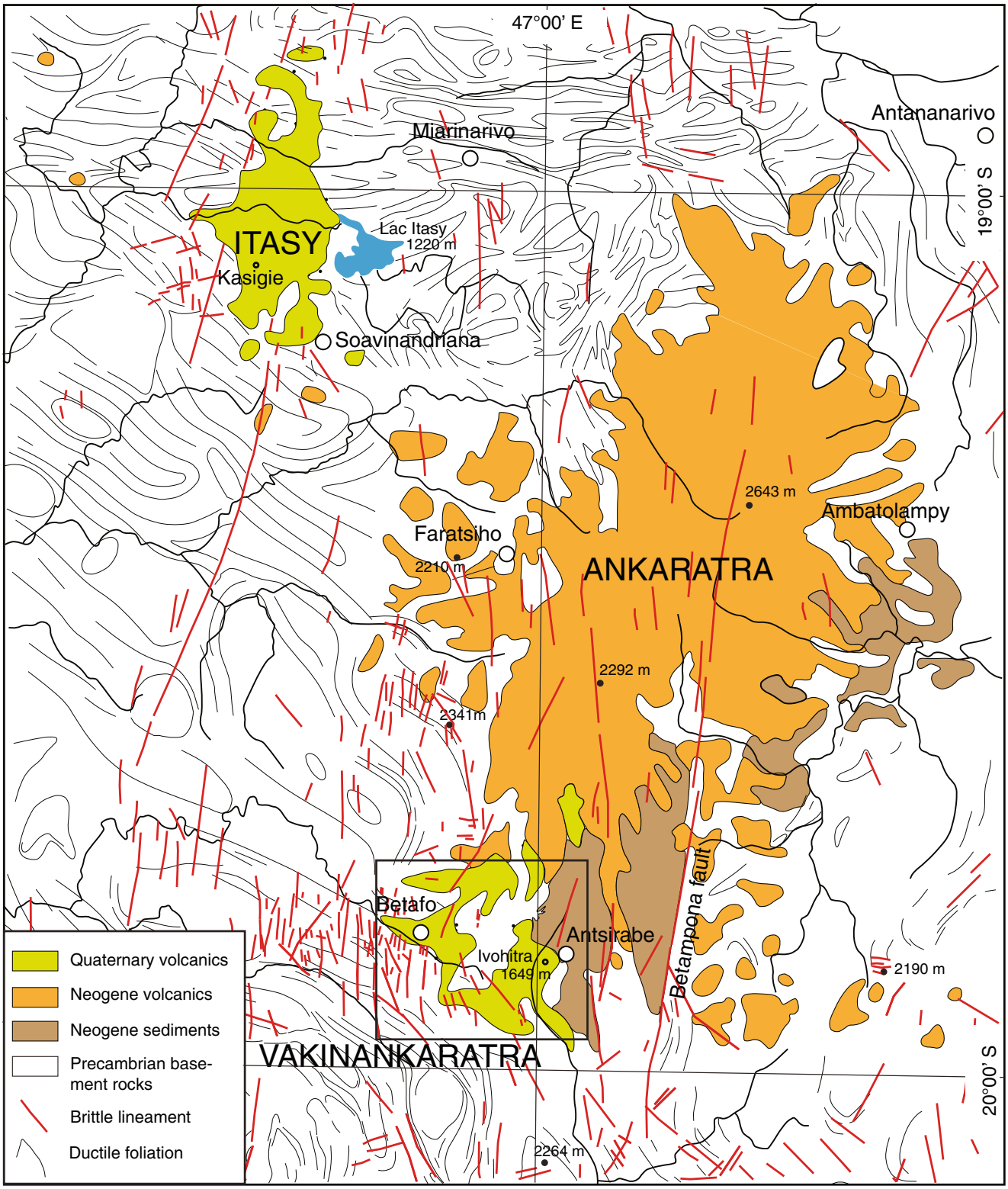

Fig. 2 Simplified geological map of the Itasy, Ankaratra, and Vakinankaratra volcanic fields in central Madagascar (after Besairie 1969). *Black rectangle* indicates the area shown in Fig. 3

The Ankaratra volcanic field covers approximately 3,800 km^2, between 18° 56′ to 19° 57′ S and 46° 46′ to 47° 30′ E, extends over 100 km in north–south direction (Woolley 2001), and has its highest elevation at 2,643 m (Fig. 2); it is dominated by basalts and andesites (Besairie 1969). Its main crest strikes NNE-SSW and continues to the south in the

Betampona escarpment, a c. 35 km long normal fault delimiting a half-graben structure containing the Ambohimiarivo basin; a N-S trending Neogene alluvial basin at an altitude of c. 1,600 m. In the northern part of the Ankaratra volcanic field, olivine melilitites and olivine nephelinites (the "ankaratrites" of Lacroix 1921–1923) are found (Woolley 2001).

Mottet (1980a, b) and Petit (1998) divide the volcanic history of the Ankaratra volcanic field into an initial phase dominated by extensive flood basalts, a second phase with emplacement of ankaratrites and trachytic extrusions, and a third phase dominated by andesitic flows, trachy-andesitic extrusions, and leucocratic tephra. Bardintzeff et al. (2010) report Oligocene, Miocene, and Pliocene K/Ar whole rock ages obtained from flood basalts of the initial phase, with the oldest age at 27.9±0.7 Ma and the youngest one at 3.11± 0.12 Ma. Mottet (1980a) gives a K/Ar age of 6.76 Ma (no error given) for a flood basalt of the initial phase and K/Ar ages of 1.71 and 1.44 Ma (no errors given) for two andesitic flows of the third phase.

While volcanism in the Vakinankaratra area is often considered to simply represent the youngest, fourth phase of the volcanic history of the Ankaratra field, it is here treated as a separate volcanic field due to its limited geographical occurrence and restricted prevalent type of eruption processes. Its surface expression consists of scoria cones, lava flows, tuff rings, and maars (Fig. 3). These volcanic rocks either overlie Precambrian basement or Neogene basalt flows of the Ankaratra volcanic field (Berger et al. 2008). Geochemical and petrological analyses indicate that the Vakinankaratra volcanic field predominantly contains tuffs and lava flows of basanitic composition with some volcanic rocks showing an evolution towards tephribasalts. Hot springs occur at several localities within the volcanic field with temperatures between 20 and 50 °C (Mottet 1980b).

Only indirect ages of volcanic deposits exist for the Vakinankaratra field. A tephra layer found at 1,175-cm depth in a drillcore from Lake Tritrivakely (Fig. 3) has been dated between 36.2±1.2 and 34.7±1 ka using radiocarbon dating on diatomaceous clay and peat layers found below and above the tephra layer (Gasse and Van Campo 2001).

Indications of phreatomagmatic activity in the Vakinankaratra volcanic field

Volcanic landforms like maars and tuff rings (cf. White and Ross 2011) attest to explosive phreatomagmatic eruption activity through interactions between magma or magmatic heat and meteoric water or the groundwater table (Schmincke 1977; Wohletz and Sheridan 1983; Wohletz and Heiken 1992; White 1996), triggering a chain of reactions resulting in almost instantaneous vaporization and volumetric expansion of large amounts of water (Sheridan and Wohletz 1981; Büttner and Zimanowski 1998). The ensuing explosions tend to form distinct deposits ranging from proximal coarse-grained to blocky, chaotic explosion breccias to more distal surge- and finer-grained airfall deposits (Wohletz and Sheridan 1983; White and Ross 2011 and references therein). Depending on the presence or absence of juvenile material in the ejecta, the eruption is distinguished to be phreatomagmatic or phreatic, respectively (Ollier 1974; Sheridan and Wohletz 1983).

In the Vakinankaratra volcanic field, which is dominated by monogenetic scoria cones and lava flows, several maar craters and tuff rings can be found. In the eastern part of the volcanic field (Fig. 3), three such craters were identified with the maar crater of Lake Andraikiba being the most prominent one and the only one containing a perennial lake. Two unnamed and—based on morphological features (White and Ross 2011)—older tuff rings are located c. 1 km east and c. 4 km southwest of Lake Andraikiba, respectively (Berger et al. 2008). To the northeast of Betafo lies Lake Tritrivakely (Fig. 3), a small crater lake filled by an ephemeral marshy lake which has been described in the literature as a maar crater (e.g., Gasse et al. 1994; Williamson et al. 1998). It should be noted that other maar craters or tuff rings might have existed in the Vakinankaratra area, whose morphology was in later stages of their volcanic activity overprinted by, e.g., scoria cones. Over wide parts of the volcanic field, laterally extensive, mostly thin, fine-grained and oftentimes larger clast bearing volcanoclastic sediments of disaggregated basement rock can be found, and these deposits provide clearly identifiable and traceable layers extending far beyond the confined eruption range of the scoria cones. While they mostly overlie palaeosoils (weathered Precambrian basement rocks or Neogene basalt flows), they are themselves overlain by basanitic-tephritic tephra and its weathered products. In the following, these deposits are described within the framework of several stratigraphic sections (Fig. 3) from four different areas of the volcanic field, and their phreatomagmatic nature is argued.

Lake Andraikiba area

Lake Andraikiba is situated approximately 7 km west of Antsirabe. It is a maar crater that is presently filled by a lake of roughly 1 km diameter (Figs. 3 and 4). The lake is reported to be "of profound depth" (Sibree 1891), but no bathymetric data is available. The crater is encircled by a ring of volcanoclastic deposits with an average height of 50 m and characterized by steep interior (~70°) and shallower external slopes (20–25°).

The general stratigraphy of the crater wall consists at the lowest part of an older basaltic flow presumably overlying the basement at the time of the Andraikiba eruption. This flow outcrops discontinuously along the lakeshore and is towards

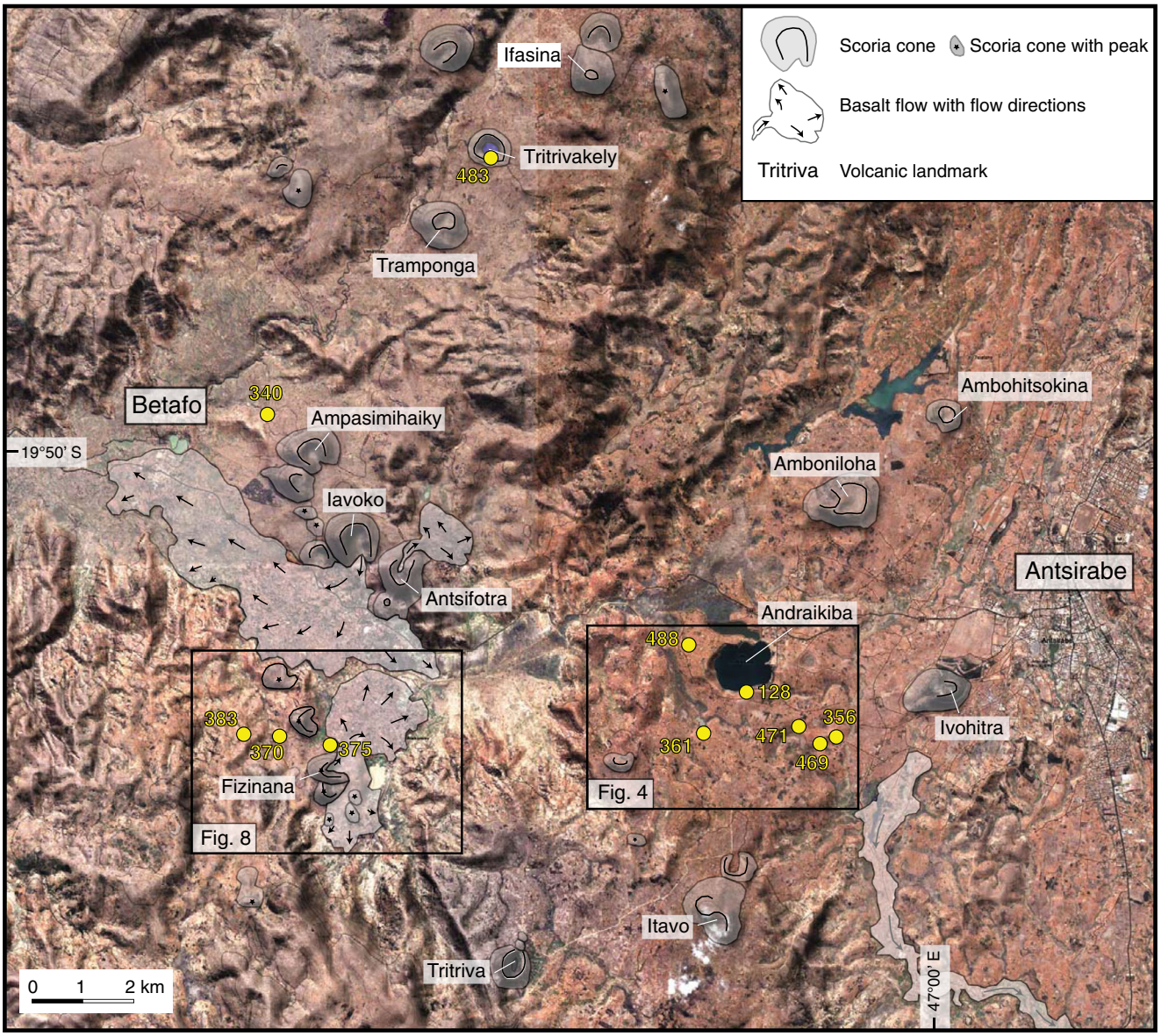

Fig. 3 Digital terrain model of part of the Vakinankaratra volcanic field showing scoria cones and basalt flows and the location of the stratigraphic sections described in the text and given in Table 1

the top strongly weathered into a thick lateritic palaeosoil of several meters thickness.

It is succeeded by a first unit of volcanoclastic material consisting of well-sorted material with rather homogeneous, sandy grain size with a granitic to granodioritic composition and no macroscopically identifiable juvenile material. Weak layering of this unit is observed in one outcrop west of Lake Andraikiba (Section 488), but in general, bedding or layering seems poor or entirely absent. The thickest deposits of this unit can be found towards the south and southwest of Lake Andraikiba, where it occurs roughly in the same topographically low position as the older basaltic flow. This is corroborated by the observed increase in thickness from Section 356 over 469 to 471 (Fig. 4), where the contact to the underlying laterized basaltic flow dips towards the west-southwest with 5 to 10°. Within less than 5 km to the south, the unit tapers out and disappears, albeit without any significant lateral granulometric gradients observable in the field. The same is observed towards the more elevated terrain west of Lake Andraikiba, where it is missing from most outcrops and consistently tracing it towards the north is hampered by extensive stretches of wetland lacking suitable outcrops. Towards its top, weathering and incipient (palaeo-)soil formation can be observed in some outcrops, forming a distinct contact to the overlying volcaniclastic breccia (Fig. 4).

This breccia makes up the largest part of the Lake Andraikiba crater rampart and forms a strongly heterogeneous deposit consisting predominantly of Precambrian crystalline

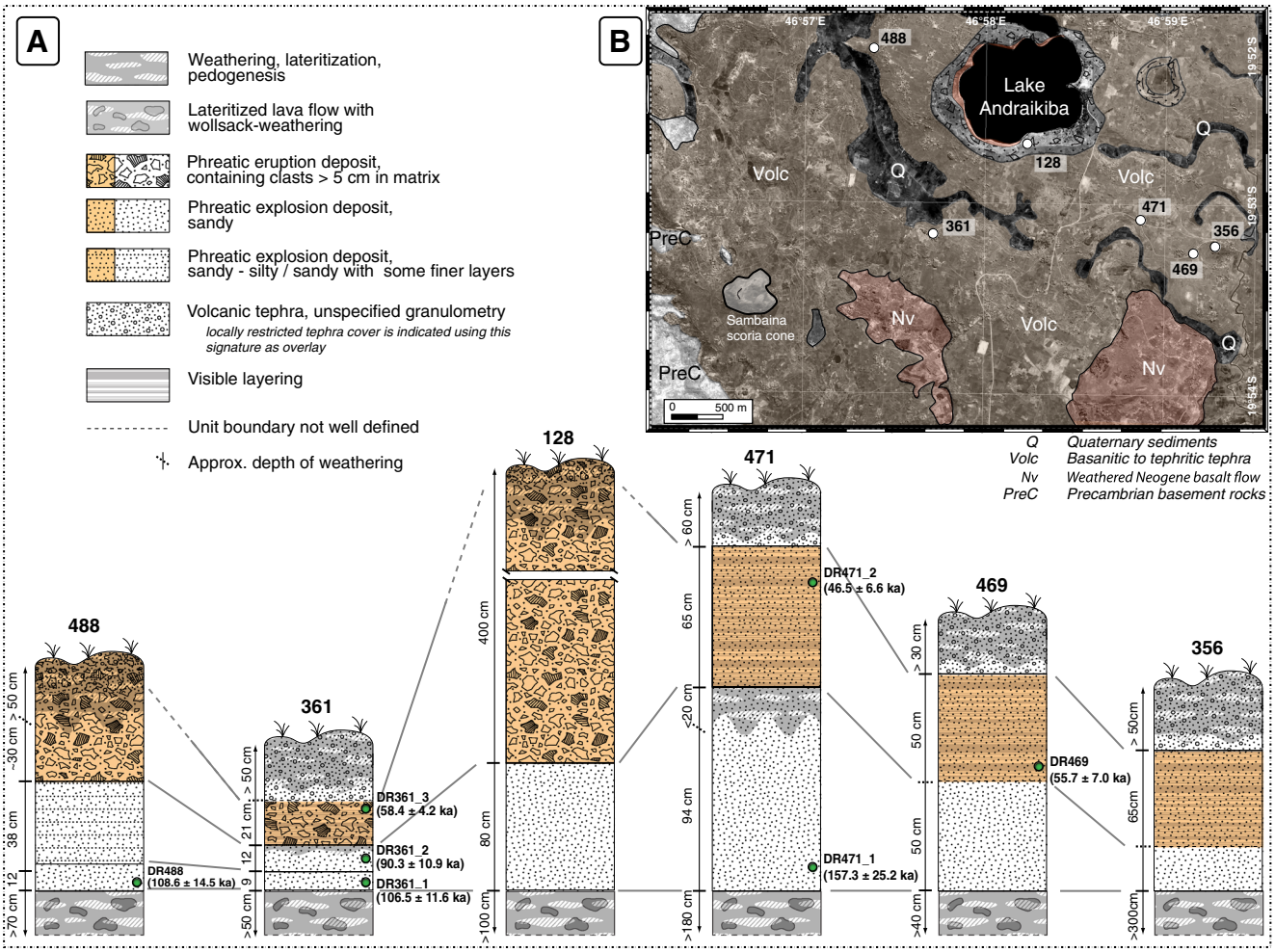

Fig. 4 **a** Stratigraphic sections of the Lake Andraikiba area. *Yellow background* indicates the main Andraikiba phreatomagmatic explosion layer. **b** Remote sensing image of Lake Andraikiba area with locations of sampled sections

basement material. It is unsorted and contains a wide range of component sizes, ranging from meter-sized blocks down to a fine-grained, sandy matrix material (Fig. 5). Only a subordinate juvenile magmatic fraction has been observed in the explosion deposits in the field. The matrix-supported, mostly angular basement clasts include primarily migmatites, quartzites, felsic gneisses, and micaschists, again representing an overall granitic to granodioritic composition. Part of these rocks show signs of calcination, which indicates elevated temperature gradients prior to the eruption (this has also been observed by Mottet 1980b). There is also a notable contribution of basaltic clasts, which originate from the explosive fragmentation of the older basaltic flow overlying the basement at the time of the Andraikiba eruption (Fig. 5). In some places, ejected basaltic blocks can be found impacted into the underlying units. With increasing distance from the crater, the relative amount and size of lithic clasts (both Precambrian basement and older basaltic material) in this unit becomes much smaller, with maximum clast size decreasing from m-sized blocks in section 128 to 30 cm in section 488 and 5 cm in section 361. To the southeast of Lake Andraikiba (sections 356, 469, and 471), the unit is almost entirely devoid of larger clasts and forms thinly layered (mm to cm scale) deposits of silty to sandy grain size with a granitic to granodioritic compositional assemblage consisting of predominantly quartz, micas, and feldspars, identical to the more proximal fine matrix material and the average composition of the crystalline clasts (Fig. 6). The difference between the more chaotic, matrix-supported, and clast-rich deposits in the outcrops to the west and southwest of the crater (sections 488 and 361, respectively) and the more homogeneous and finer-grained, layered outcrops towards the southeast could be caused by a directional blast during the eruption. In general, the radial decrease in clast size is accompanied by an overall increase in the degree of layering, and—especially in the southeastern direction—a rapid proximal reduction in overall thickness of this unit. This, together with the concordant stratigraphic position and its traceability and correlation from distal to proximal outcrops allow the source of this unit to be traced back to Lake Andraikiba (Fig. 4) and suggest that it was formed during the main maar-forming eruption.

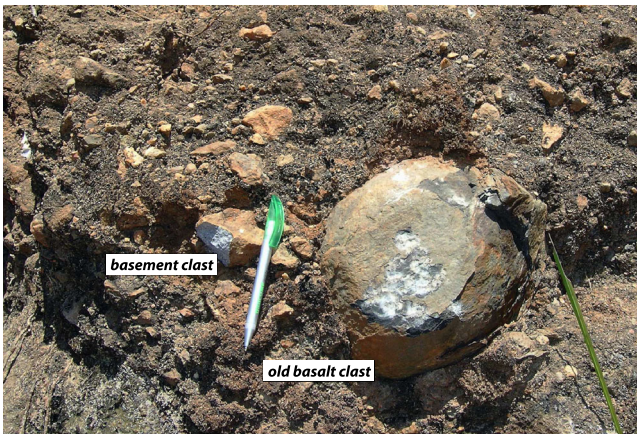

Fig. 5 Outcrop photograph of the main Andraikiba explosion breccia with clearly visible subangular clasts of crystalline basement and the old basalt flow. The matrix-supported deposit is unsorted, shows a wide range of particle sizes, and is predominantly composed of crystalline basement lithics and reworked material from the underlying old basalt flow. The photograph was taken on the inner rampart of the Lake Andraikiba crater, near section 128

Along the crater rampart, the explosion breccia is stratigraphically followed by a more tephra-rich pyroclastic deposit, consisting of multiple cm to dm thick layers of strongly heterogeneous grain size varying between dark ash and lapilli. It contains a substantial amount of angular to subrounded clasts of up to 40 cm from the crystalline basement and from the old basalt flow. The dominant size fraction of these clasts is in the range of 5–15 cm; the larger part of them aligned parallel to the bedding (Fig. 7). Along the inner wall of the rim, the orientation of the bedding is towards the crater center, indicating a

Fig. 6 Close-up outcrop photograph of the layered upper sandy explosion deposit at section 471, southeast of Lake Andraikiba, immediately prior to sampling of sample DR471_2. The coin is approximately 2.5 cm in diameter

Fig. 7 Outcrop photograph of the uppermost pyroclastic unit at Lake Andraikiba. The deposit contains a large number of lithics (from the crystalline basement and the old basaltic lava flow), most of them showing bedding parallel alignment. Outcrop situated on the external side of the rim, near section 128

deposition on an existing rampart morphology. This unit crops out discontinuously and with strongly variable thickness along the crater rim and is mostly preserved on the less steep parts towards the top and along the outer flank of the rim. With increasing radial distance from the crater, the fraction and size of larger clasts decreases rapidly, and they practically disappear over a distance of less than 700 m. In the more distal sections to the southeast of the crater, this unit is comprised mainly of small lapilli with average grain size below 1 cm, forming rather homogenous, nonlayered deposits of roughly half a meter thickness, which are significantly affected by weathering and lateritic pedogenesis. The contact to the underlying unit is fairly sharp in the distal sections but is far less distinct closer to and on the crater rim. It appears that these deposits represent a later stage of the eruptive cycle at Lake Andraikiba, in which the initial explosive activity changed towards a potentially less violent, more strombolian type.

Lake Tritrivakely

Lake Tritrivakely, approximately 9 km northeast of Betafo (Fig. 3), is a maar crater containing an ephemeral lake of approximately 300 m in diameter. Estimates of the sedimentary infill vary between 50 (Sifeddine et al. 1995) and 90 m (Gasse and Van Campo 2001). With the exception of the southeastern side, the crater is encircled by a 50–80 m high basaltic tuff ring with the higher rampart along the northern side featuring steep interior slopes over 45° and a lower rim towards the south and southeast of significantly shallower dip on the inner flank. Numerous angular blocks of migmatitic composition up to 1 m in diameter, with the majority measuring in the decimeter range, as well as prevalent volcanic bombs and basaltic blocks

of similar sizes can be found on both the interior and exterior slopes of the crater. The juvenile material consists of olivine-pyroxene basalt and some of the larger volcanic blocks contain crystalline xenoliths of migmatitic composition, very similar to the crystalline basement blocks. According to Mottet (1980b), the migmatitic composition corresponds to the Vavato migmatites which constitute the basement in the region.

Two separate units of predominantly sandy grain size, consisting primarily of quartz, feldspar, and partially oxidized reddish mica and rare basaltic clasts (<5 mm) were identified in several outcrops along the inner part of the southern rim. The upper unit has a thickness of approximately 60 cm and exhibits banking on a cm scale, while the lower one is far less structured and exceeds 1 m in thickness. On the steeper parts of the crater wall, no clearly identifiable remains of these deposits can be found. Due to the absence of large clasts, their small, fairly homogeneous grain size, and near-identical appearance to the distal outcrops of the basement rich, sandy volcanoclastic units observed at Lake Andraikiba, these deposits are interpreted as being of external volcaniclastic origin from an as yet undetermined source.

Fizinana and Ampasamihaiky areas

The Fizinana and Ampasamihaiky volcanic complexes are situated 6 km southeast and 2 km east of the town of Betafo, respectively (Fig. 3). The twin scoria cones of the Ampasamihaiky volcanic complex are considered to be among the oldest volcanic edifices in the region of Betafo (Mottet 1980b). Towards the southeast, we find the Iavoko and Antsifotra volcanic complexes, whose significantly reduced morphological degradation clearly indicates younger ages compared to Ampasamihaiky, with the Antsifotra being the youngest one of the group. Both complexes have associated basanitic flows, with the flow emanating from the main Iavoko scoria cone extending over a distance of c. 8 km, predominantly towards the northwest into the Betafo basin. To the south, the Fizinana volcanic complex is dominated by two large scoria cones (Fig. 8), with the younger northern one being presumably similar in age to the Iavoko scoria cone (Mottet 1980b). The Fizinana area also features quite a large number of smaller cones, ranging from morphologically far older cones to small secondary vents seemingly contemporaneous to the main Fizinana cones. The Fizinana complex sources basaltic to basanitic effusiva, which flow towards the north, where they encounter the Iavoko flow.

Most of the outcrops near the Fizinana and Ampasamihaiky volcanic complexes contain at least two units which are of a similar type as the sandy, basement material-rich volcaniclastic deposits described in the other areas. Being anterior to the large lava flows in the Betafo region, however, these units could not be continuously traced between the two areas. In all observed outcrops, the lowermost of these deposits directly overlies an old basement laterite with a thickness of at least several meters, indicating that phreatomagmatic volcanic activity occurred after a prolonged phase with no volcanic sedimentation in these areas.

In the Fizinana area (sections 383, 370, and 375; Fig. 8), the stratigraphically lowest deposit consists of approximately 60 cm of poorly sorted, sandy to coarse sandy material (Fig. 9), in places containing subordinate rock fragments up to a few centimeters. Both the clasts and the matrix material are of granitic to granodioritic composition, representative of the crystalline basement in the area. In the field, no volcanic material was observed in this unit, but the potential presence of a minor fraction of volcanic ash or small lapilli cannot be excluded. Bedding is poor or almost entirely absent in most of the outcrops. This lower unit is overlain by a fines-depleted dark gray to black lapilli tephra with particle sizes predominantly between 0.5 to 2 cm and an average thickness of approximately 20 cm. In general, the deposit shows no bedding, with the exception of section 370, where the deposit is interrupted towards the top by an approximately 5 cm thin layer of more brownish lapilli with average size of <0.5 cm and more fine-grained matrix material (Fig. 9). At the base of this tephra, small basement clasts up to several centimeters in size occur. Based on an increase in thickness of this deposit and an increase in relative amount and size of the basal crystalline clasts, the source of this deposit is tentatively linked to an older scoria cone immediately north of the Fizinana volcanic complex (Fig. 8).

Overlying the tephra is a second, 10 to 20-cm thick, finely laminated, sandy unit with predominantly basement composition and a subordinate amount of small lapilli in the size range of a few millimeters (Fig. 9). This unit has only been identified in the three sections 383, 370, and 375 (Fig. 8), and its extent or stratigraphic role is unclear.

Following a homogeneous sequence of moderately well-sorted darker lapilli with average grain size of approximately 1 cm, the Fizinana area features an upper unit composed of well-sorted, finely laminated sandy material of identical basement composition as the underlying such deposits but with no clearly discernible volcanic fraction (Fig. 9). This upper unit is ubiquitously capped by tephra deposits which can be traced to the younger of the main Fizinana scoria cones, where they form the latest, cone-forming pyroclastic deposit. This is supported by larger blocks of crystalline material up to several decimeters in size which can infrequently be found at section 375 and other outcrops proximal to this cone. Some of these clasts impacted the upper sandy deposit (Fig. 10), but their size and occurrence is gradually reduced with increasing distance from the cone, and at section 370, crystalline material in the covering tephra is rare and does not exceed the grain size of the lapilli.

In the Ampasamihaiky area (section 340; Figs. 3 and 11), a lower and only a few centimeter-thick deposit of thinly layered sandy material comprised primarily of quartz, feldspar, mica, pyroxene, and subordinate hornblende grains directly

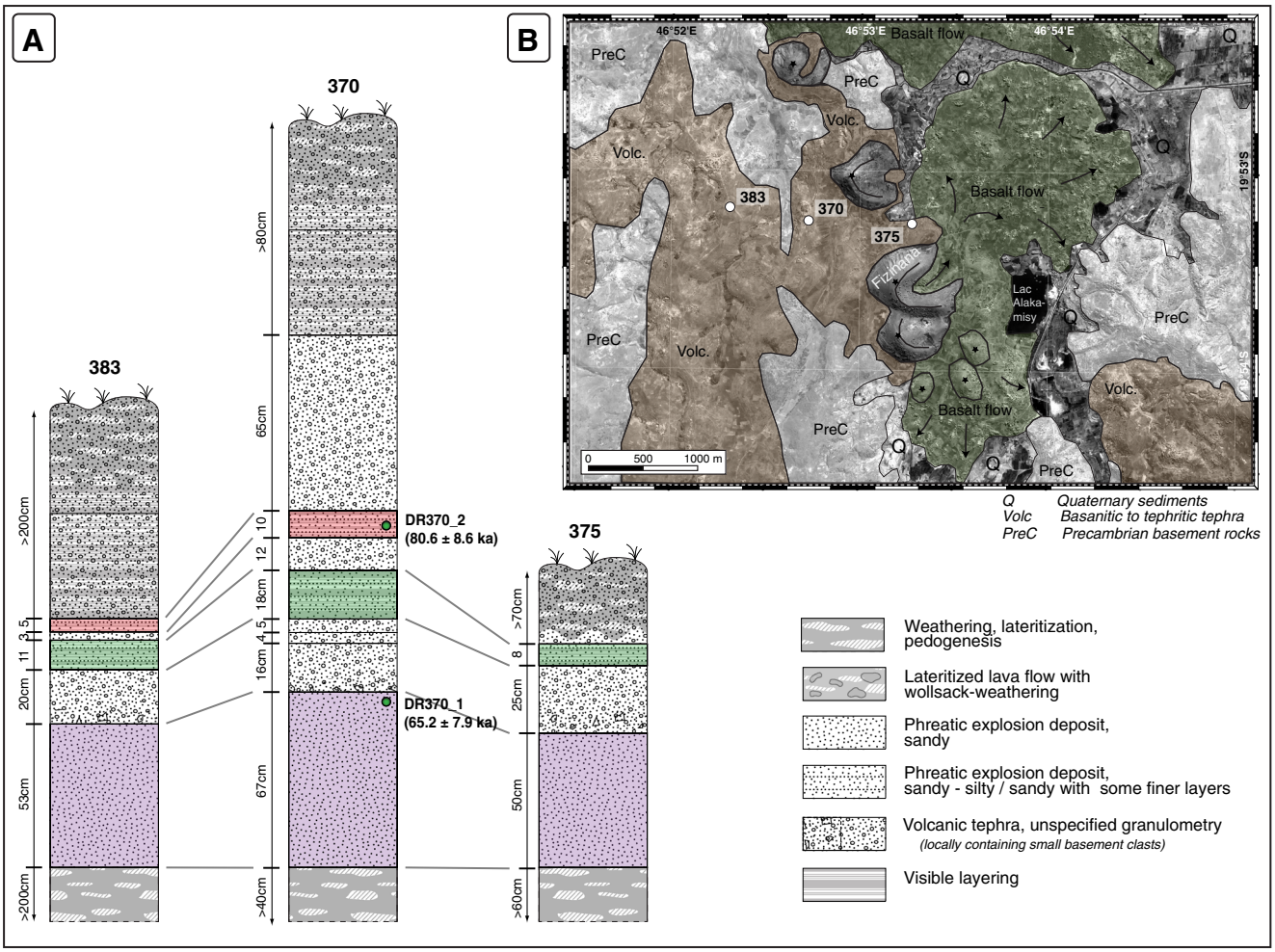

Fig. 8 **a** Stratigraphic sections of the Fizinana area. *Colored layers* represent units that can be stratigraphically correlated. **b** Remote sensing image of Fizinana area with locations of stratigraphic sections

overlies a massive laterite exceeding several meters in thickness (Fig. 12). As such, it lies in comparable stratigraphic position as the basal deposit of comparable type observed at the Fizinana complex. It is followed by a series of tephra and light brown to ochre colored volcanic ash layers, none of which contain basement clasts or volcanic bombs. The mostly homogeneous dark to black tephra layers show a predominant grain size between 0.5 and 3 cm, are mostly homogenous, and only exhibit minor bedding in the slightly more brownish bottom part. Towards the top, the tephra is weathered to variable depths and forms a brownish palaeosoil (Fig. 12). The tephra and ash sequence most probably originates from the Ampasamihaiky cone (Fig. 3), as this stratigraphic succession can be traced upslope featuring increasing thickness and grain size in the tephra layers. Overlying the palaeosoil of the Ampasamihaiky tephra is an upper deposit of fine sandy to silty layered material of variable thickness of around 10 cm (Fig. 12). It is of similar composition as the lower such unit, albeit of slightly finer grain size. It is in turn capped by another sequence of dark tephra, interspersed with layers of finer, volcanic ash, grading up into the thin modern soil (Fig. 12). Most likely, the uppermost tephra layers originate from the nearby young Iavoko and Antsifotra scoria cones (Fig. 3).

The geographic sources of the eruption events that produced the sandy, basement material-rich eruption units observed near the Fizinana and Ampasamihaiky volcanic complexes are not clear. The generally elevated thickness between 25 and 67 cm and the occurrence of small clasts in the lowermost such unit in the Fizinana outcrops indicate a more proximal setting compared to the only 2–5 cm thickness in the assumedly corresponding unit in the Ampasamihaiky area (Fig. 11).

The sandy deposits from all locations described above show lithological compositions dominated by fractured basement material, both as the fine, sandy matrix material and as the prevalent lithological type of embedded larger clasts, and a rather homogeneous, generally small grain size of the fine material together with an often layered or thinly bedded structure. In the case of the Lake Andraikiba deposits, geometrical properties such as accommodation of deposit thickness to preexisting topography and lateral thinning can be observed,

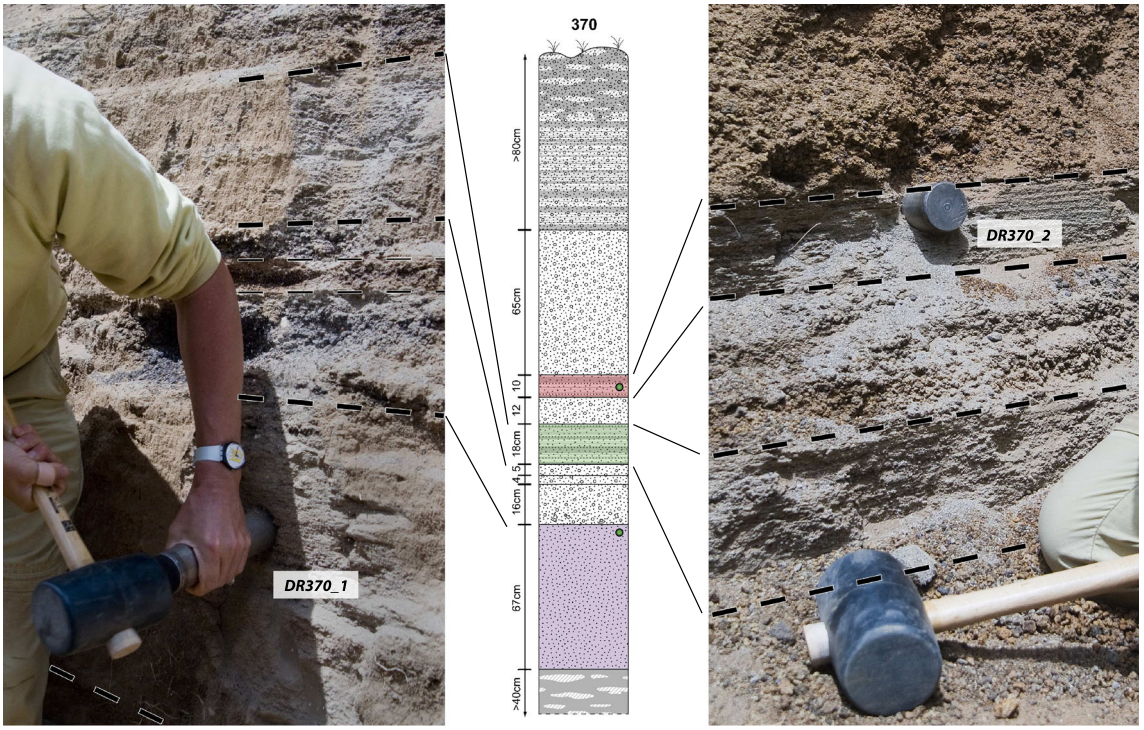

Fig. 9 Outcrop photograph and stratigraphic profile of section 370 in the Fizinana area, with sampling locations of samples DR370_1 and DR370_2. The photographs also illustrate how samples were extracted using a steel tube to prevent accidental bleaching of the luminescence signal by daylight

and the distal sandy units can directly be traced back to the maar crater and the deposits which form the bulk of the crater rim. In both the Andraikiba and Fizinana area, lateral changes in frequency and maximal size of embedded larger clasts are noted. Based on these aspects, we interpret these clearly identifiable deposits as being of phreatomagmatic origin.

Fig. 10 Lithic clast impacted into a sandy explosion layer near section 370 in the Fizinana area. The trajectory of the block indicates that it originated most likely from the main Fizinana scoria cone, south of this location

With the bulk of the material of these deposits derived from Precambrian granitic to granodioritic basement rocks, most of the quartz and K-feldspar grains in these sediments are of plutonic origin, with no or only a very minor contamination by volcanic quartz and K-feldspar grains, respectively, due to the overall basaltic to tephritic/andesitic petrology of the juvenile volcanic material.

Methodology

Luminescence dating

Luminescence dating techniques allow the determination of the time that has elapsed since quartz or K-feldspar grains have last been exposed to daylight, heat, or mechanical stress. When undisturbed, the sample accumulates a signal induced by natural radioactivity, both ambient and internal (in the case of K-feldspar) as well as from cosmic radiation. The ionizing radiation causes excitation of atoms within the crystal lattices of the mineral grains, leading to the formation of activated electrons at higher energy states and a corresponding electron hole. While the majority of these electrons fall back and recombine instantaneously, some are captured at lattice

Fig. 11 Comparison of section 370 from the Fizinana area with section 340 from the Ampasamihaiky area. The Ampasamihaiky section is not to scale, but the sampled phreatomagmatic layers are 2–5-cm (DR340_2) and 5–15-cm thick (DR340_1). Legend as in Fig. 8 ▶

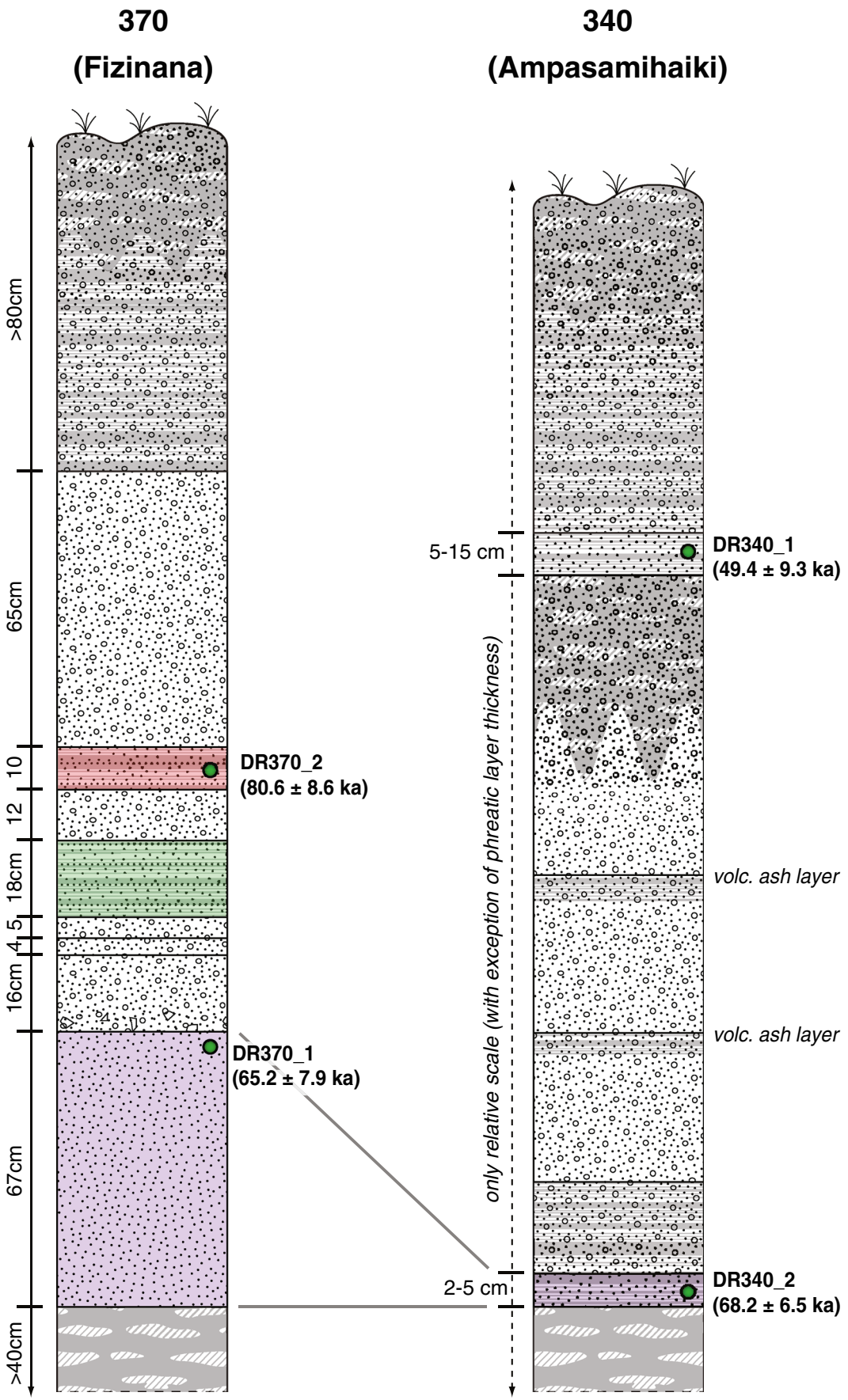
370
(Fizinana)
340
(Ampasamihaiki)
>80cm
65cm
10
12
18cm
4
5
16cm
67cm
>40cm
DR370_2
(80.6 ± 8.6 ka)
DR370_1
(65.2 ± 7.9 ka)
5-15 cm
DR340_1
(49.4 ± 9.3 ka)
volc. ash layer
volc. ash layer
only relative scale (with exception of phreatic layer thickness)
2-5 cm
DR340_2
(68.2 ± 6.5 ka)

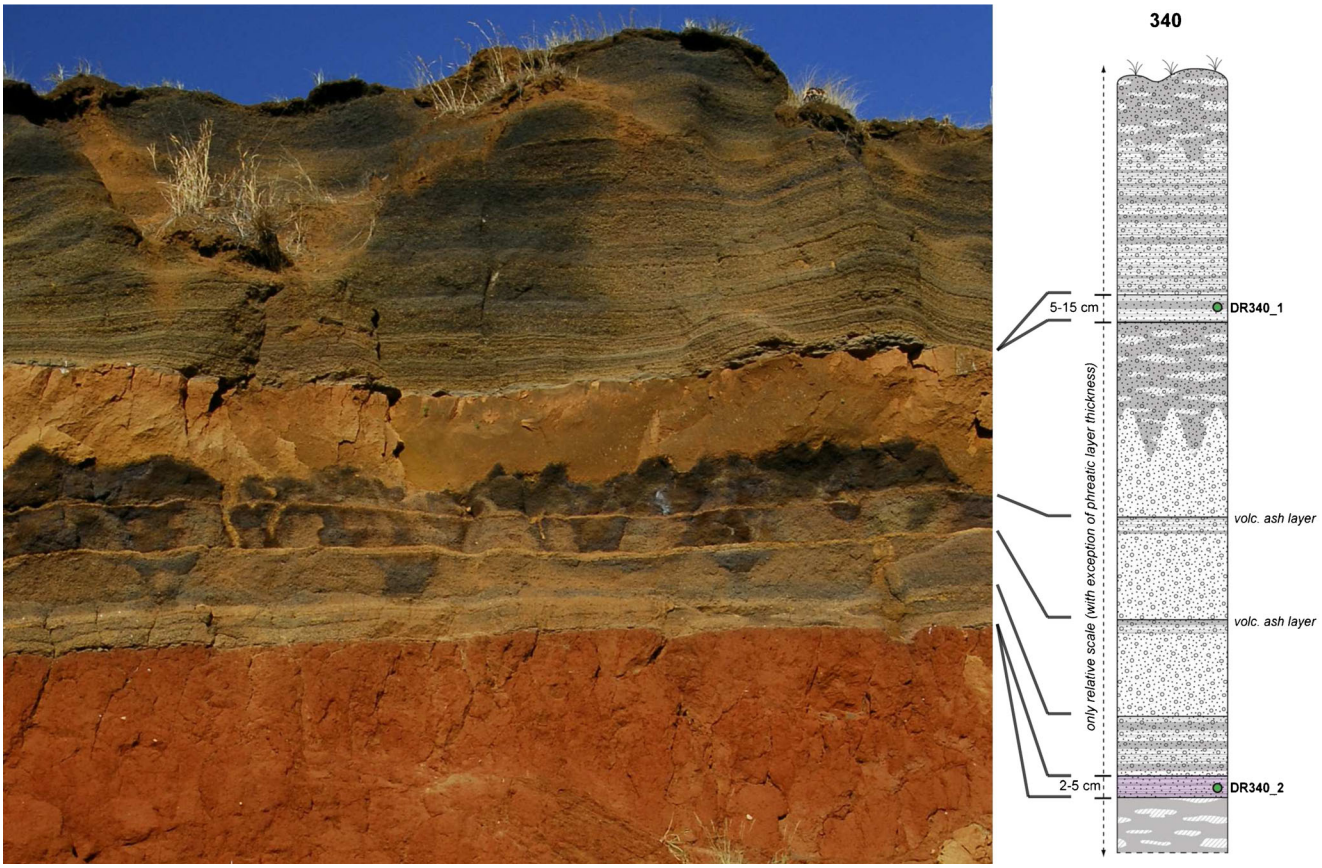

Fig. 12 Outcrop photograph and stratigraphic profile of section 340 in the Ampasamihaiky area, with indication of the layers in which samples DR340_1 and DR340_2 were taken

defects, so called electron traps. While energetically shallow traps can only keep their charge for a short amount of time, the electrons in deeper traps remain stable over geological timescales, leading to an accumulation of filled traps. When exposed to a particular stimulation energy (e.g., light, heat, or mechanical stress), these trapped electrons can escape the energy trough of the trap and recombine with an electron hole under emission of the stored energy in the form of luminescence. Based on the form of stimulation, optically stimulated luminescence (OSL), infrared-stimulated luminescence (IRSL), thermoluminescence (TL), and mechano-luminescence are differentiated. Any measured luminescence signal is therefore representative for the amount of traps filled since the last resetting. After measuring the natural luminescence signal of a sample, it is repeatedly

Table 1 Location of luminescence samples

Section	Samples	Coordinates (WGS 1984 UTM, Zone 38S)	Elevation (m.a.s.l.)
Pt. 340	DR340_1	19° 49.793′ S, 46° 52.578′ E	1,540
	DR340_2		
Pt. 361	DR361_1	19° 53.161′ S, 46° 57.718′ E	1,560
	DR361_2		
	DR361_3		
Pt. 370	DR370_1	19° 53.251′ S, 46° 52.727′ E	1,600
	DR370_2		
Pt. 469	DR469	19° 53.249′ S, 46° 59.159′ E	1,511
Pt. 471	DR471_1	19° 53.074′ S, 46° 58.860′ E	1,539
	DR471_2		
Pt. 483	DR483_1	19° 46.796′ S, 46° 55.201′ E	1,800
	DR483_2		
Pt. 488	DR488	19° 52.195′ S, 46° 57.382′ E	1,552

bleached, irradiated, and measured with increasing radiation doses, resulting in an internal signal/dose calibration curve. This allows the calculation of the palaeodose (D_e), which was required to produce the initially measured natural luminescence signal. Using gamma-spectrometry, for example, the dose rate (D*) to which the sample was subject can be determined, based on which the age (T) of the last resetting event can be calculated as $T=D_e/D^*$. A comprehensive overview of luminescence dating methods is given in Preusser et al. (2008).

Since the early 1970s, several studies have aimed at dating volcanic deposits using luminescence methods, but anomalous fading (a signal instability causing age underestimation) has been reported for both volcanic feldspars (e.g., Wintle 1973), and volcanic quartz (Bonde et al. 2001; Tsukamoto et al. 2007). While Fattahi and Stokes (2003) summarize good consistency of TL ages with independent age control, problems with anomalous fading occurred in many other studies. An approach to overcome this problem could be the use of the red emissions, which have proven to be more stable than other TL emissions (e.g., Fattahi and Stokes 2000; Ganzawa et al. 2005; Bassinet et al. 2006). However, relatively little research has been carried out, and to date, only a few research groups have focused on this topic.

Recently, Rufer et al. (2012) proposed new approaches for dating young volcanic eruptions by luminescence methods. They argued that country rock fragmented by phreatic or phreatomagmatic eruptions undergoes complete mechanical resetting of luminescence signals and hence that such materials are potentially suitable for direct dating (Fig. 10). The main advantages of this approach are, firstly, that it enables the dating of volcanic by-products that do not contain juvenile minerals, and, secondly, that nonvolcanic quartz and K-feldspar are known to be not or at least less affected by anomalous fading. This innovative approach was successfully tested by Preusser et al. (2011), who directly dated such volcaniclastic deposits from Late Quaternary eruptions in the Eifel volcanic field, and whose ages are independently well constrained by indirect dating methods such as radiocarbon and varve chronology.

One potential problem with this approach could be an incomplete resetting of the luminescence signal during the eruption, leading to age overestimation. To investigate this issue, several aliquots are measured per sample, where the signal from each aliquot is considered to originate from not more than a few grains. The spread of repeated measurements is then used to evaluate whether or not the signal has been equally erased in all grains during the eruption.

Sampling, sample preparation, and experimental parameters

Samples for luminescence dating were taken from clearly identified phreatomagmatic eruption deposits (Fig 3; Table 1) containing large amounts of mechanically fractured quartz and feldspar grains and negligible juvenile magmatic material. The fractured grains originate from Precambrian orthogneisses and granitoids that form the country rock in the Vakinankaratra region. We sampled the fine sand grain-size fraction of the eruption deposits (Fig. 13) by driving a steel tube into the sediment in order to retrieve material without exposing it to light (Fig. 9). The sample was then carefully transferred to light-tight bags and kept in the dark until its processing in the lab.

Sample processing and measurements were carried out under subdued red light. After gravimetric determination of the moisture content, the samples were dried, sieved, and the 100–150-μm size fraction was selected for further processing. Subsequent to the removal of the magnetic fraction with a neodymium hand magnet, the samples were subjected to a 10 % hydrochloric acid and a 35 % H_2O_2 wash in order to remove carbonate and organic material. A two-step density separation using LST (a solution of lithium heteropolytungstates in water with specific gravities of 2.58 and 2.70 g cm^{-3}, respectively) was employed to isolate the quartz and K-feldspar fractions, with the quartz being subsequently etched in 40 % hydrofluoric acid (Mejdahl 1985). The quartz separates were further treated with hydrofluorosilicic acid (H_2SiF_6) for 1 week in order to eliminate any remaining feldspar contamination (Steffen et al. 2009). No acid etching was done on the K-feldspar separates because this would most probably not remove a uniform surface layer (Duller 1992). An alpha efficiency value of 0.07±0.02 was assumed (Preusser 1999).

Measurements were carried out on Risø DA-20 TL/OSL readers fitted with internal $^{90}Sr/^{90}Y$ beta sources. IRSL signals were detected using a Schott BG39 and a LOT/Oriel D410/30 filter combination, whereas a Hoya U340 UV-transmitting filter was used for OSL detection. For the K-feldspar samples, D_e was determined following the single-aliquot regenerative-dose (SAR) approach of Wallinga et al. (2000). The samples were stimulated by IRSL diodes at 40 °C for 300 s (Fig. 14) and the initial 25 s of the measurement were used. Background subtraction was made using the last 25 s. Based on preheat tests, a preheat temperature of 290 °C was chosen and subsequently applied for either 10 or 60 s on both regenerative and test dose. No influence of preheat time on the measured D_e could be determined except for three samples (DR471_2, DR340_1, and DR483_2), where the deviation is probably the result of poor statistics of the 60-s preheat D_e determination due to a low number of aliquots (Fig. 15; Table 2). As a consequence, ages in the text are given as averages of the two types of measurements as indicated by the column Age_{avg} in Table 2. Dose recovery tests all yielded a recovered dose within 10 % of the given dose.

For quartz OSL, shine-down curves reveal a notably slower decay and higher overall background compared to the signal decay behavior of Risø calibration quartz, a well-behaving sample dominated by a fast component. As feldspar

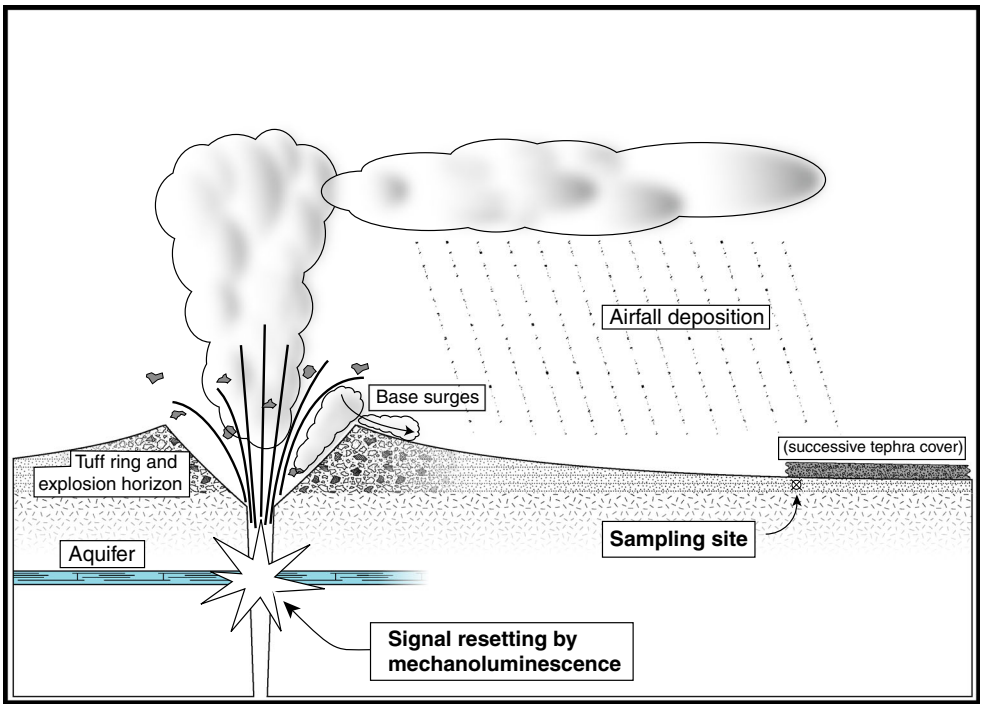

Fig. 13 Schematic section through a maar crater showing relevant processes for luminescence dating of phreatomagmatic deposits as well as possible sample sites

contamination can be excluded due to the chemical treatment of the quartz separates, the curves most likely indicate a relatively weak or absent fast component (cf. Steffen et al. 2009). In order to circumvent problems with the quartz samples as described by Steffen et al. (2009), all data presented in this paper are from K-feldspar IRSL measurements.

Environmental dose rates

Assessment of environmental (external) dose rates was done by high-resolution gamma spectrometry measurements of ^{40}K, ^{238}U, and ^{232}Th series nuclide concentrations in material taken from the immediate surroundings of the luminescence samples. For samples taken from deposits less than 30-cm thick and for samples taken near the contact to another layer, the adjacent layers were sampled as well and their influence on the dose rate was taken into account using the infinite-layer model built into the ADELE software (Kulig 2005). This is particularly important because of significant differences in radionuclide composition between phreatomagmatic deposits, underlying palaeosoils, and overlying tephra. Cosmic dose rate was calculated based on present-day overburden at each sampling site.

As water attenuates the environmental dose rate, a reliable estimate of the moisture content of the material surrounding the luminescence sample is necessary for accurate age determinations. While the moisture content of a material at the time of sampling can easily be determined gravimetrically, estimating a time-integrated water content spanning the entire time range of the sample since its deposition is more difficult. As our samples were taken at the end of the dry season, we use the actually measured moisture content ($moist_{meas}$) as the minimal boundary condition (Table 2). The gravimetrically compacted samples were saturated with water and let to drip through a

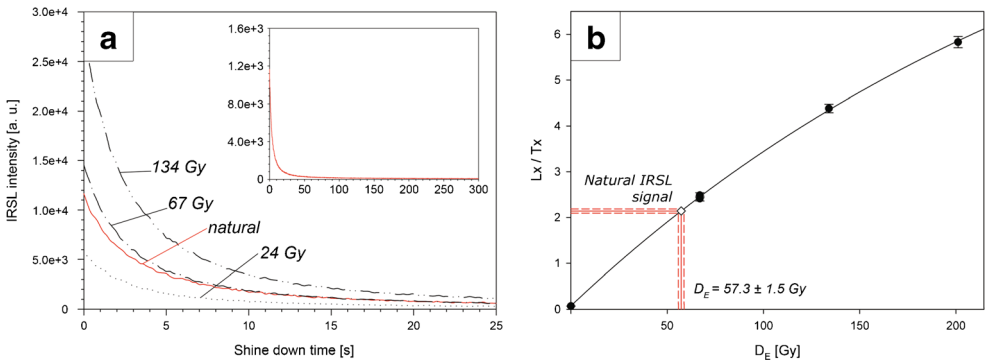

Fig. 14 **a** Representative IRSL decay curve (sample DR483_1) for the natural and three regenerative doses, given in the initial 25-s signal integral used for the measurements. *Inset* natural signal plotted over the entire 300-s stimulation time. **b** Typical IRSL dose response curve (sample DR483_1)

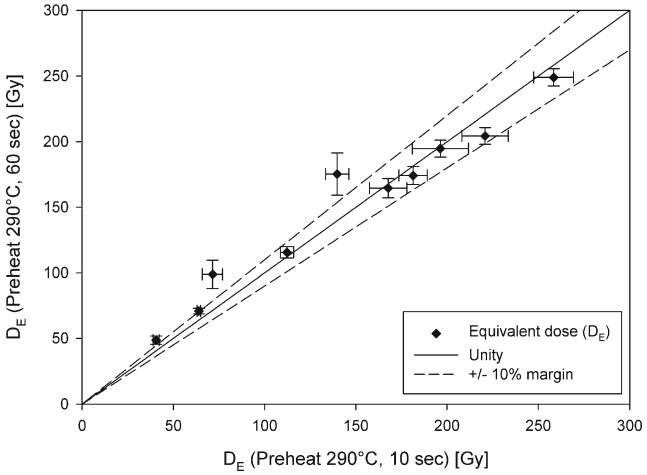

Fig. 15 Comparison of D_e obtained for preheating at 290 °C for 10 and 60 s, respectively, shows an overall good fit close to unity. The three outlying samples above the 10 % discrepancy margin all have a low number of aliquots measured for the 60-s preheat (DR483_2, DR340_1, DR471_2)

sieve for several hours in order to measure the retained capillary water content. This is not directly comparable to a true determination of the sample's field capacity (Israelson and West 1922) and overestimates the water content due to factors like sample disturbance and shortened drainage time (normally 2–3 days). However, the obtained values of 36–47 % H_2O for saturation content are in an acceptable range for sandy soils and the drained values of 23–29 % are therefore taken as conservative maximum values for water content in the field under wet conditions. Furthermore, Randriantsoa (2001) reports water saturation levels dropping to 75 % of near-surface values at depths larger than 10 cm for volcanic soils in the region of Betafo during the wet season. This was taken into account and maximum moisture ($moist_{max}$) contents were taken as three quarters of the drained water content (Table 2). Pluviometric data given for the meteorologic station in Antsirabe show a 25-year-averaged annual rainfall of 1,466 mm with 87 % of precipitation during the wet season between mid-October and mid-April (Zebrowski and Ratsimbazafy 1979). Based on these numbers, annually averaged water contents ($moist_{avg}$) were calculated as $(6\times moist_{meas}+6\times moist_{max})/12$ and assigned an estimated ±5 % uncertainty (Table 2). These numbers were subsequently used in the age calculations.

Determination of internal potassium content of the K-feldspar separates

Each sample was analyzed on a Zeiss EVO 50 XVP scanning electron microscope using energy dispersive X-ray (EDX) spectroscopy. K-feldspar grains were identified optically using a combination of backscattered electron (BSE) imaging and EDX element mapping of K, Na, and Ca in order to distinguish them from, e.g., plagioclase. Element mapping indicates that Na- and Ca-feldspars are only minor constituents relative to K-feldspar. Multiple EDX measurements were then taken on several K-feldspar grains per sample to determine the average internal potassium content in the K-feldspars of that sample (given as K_{Fsp} in Table 2). It is noted that most

Table 2 Summary of dosimetric data for IRSL

Area		Sample	K_{Fsp} [a] (%)	K (%)	Th (ppm)	U (ppm)	$Moist_{meas.}$ [b] (%)	$Moist_{avg.}$ [c] (%)	Depth (m)	D_{Fsp} [d] (Gy ka^{-1})
Lake Andraikiba	Lower Upper	DR361_3	12.5±0.6	0.84±0.02	21.91±0.26	7.13±0.05	7.7	12.5±2.5	0.50	4.51±0.41
		DR471_2	9.5±1.0	1.05±0.02	20.53±0.45	3.80±0.06	7.6	13.5±2.7	0.75	3.72±0.43
		DR469	11.2±1.0	1.00±0.03	20.97±0.80	4.20±0.13	10.5	15.5±3.1	0.85	3.80±0.34
		DR488	9.0±1.4	0.24±0.01	4.54±0.28	7.74±0.08	18.7	20.2±4.0	0.90	3.08±0.28
		DR361_2	10.5±0.8	0.23±0.01	5.88±0.24	4.77±0.05	5.4	11.4±2.3	0.71	2.70±0.27
		DR361_1	11.4 ± 0.9	0.23±0.01	4.63±0.16	5.56±0.03	18.7	20.0±4.0	0.80	2.60±0.21
		DR471_1	10.9 ± 1.6	0.22±0.01	6.56±0.23	1.54±0.05	7.9	13.7±2.7	2.10	1.94±0.22
Ampasimi-kaiki		DR340_1	11.4±1.3	0.41±0.01	7.99±0.19	0.96±0.05	3.1	11.8±2.4	0.20	1.79±0.27
		DR340_2	11.6±0.6	0.76±0.02	6.04±0.20	0.89±0.04	9.2	14.8±3.0	2.00	2.09±0.16
Fizinana		DR370_2	11.3±0.6	1.37±0.03	7.79±0.11	1.47±0.03	4.6	14.8±3.0	1.45	2.46±0.19
		DR370_1	8.4±0.5	1.73±0.04	11.25±0.19	2.37±0.05	3.5	14.2±2.8	2.10	3.08±0.28
Lake Tritrivakely		DR483_2	11.8±0.1	1.80±0.04	4.20±0.19	0.60±0.02	8.5	14.1±2.8	0.80	2.56±0.22
		DR483_1	9.9±1.1	2.10±0.04	4.10±0.11	0.50±0.01	11.3	15.5±3.1	2.30	2.63±0.17

[a] Internal K concentration of the sample's K-feldspar grains

[b] Gravimetrically measured moisture content of the sample at time of sampling (end of dry season)

[c] Average moisture content of the sample; used for age determinations. For calculation see text

[d] Total dose rate used for age determinations; includes internal, environmental (including layers), and cosmic dose rate

of these values are slightly lower than the value of 12.5±0.5 % suggested by Huntley and Baril (1997) and often found in the literature as a surrogate value.

Correction for anomalous fading

It is a known phenomenon in luminescence dating of feldspars that the true age of samples can be underestimated due to continuous loss of signal over time, a process called anomalous fading (Wintle 1973). Various approaches to determine the rate of this signal loss, expressed by the *g* value (Aitken 1985), and to calculate corrected ages have been proposed (e.g., Huntley and Lamothe 2001; Lamothe et al. 2003; Wallinga et al. 2007; Kars et al. 2008). In this study, fading-corrected ages were calculated after Huntley and Lamothe (2001). Due to analytical problems, *g* values could only be obtained for samples DR488 (3.0±0.7 %/decade), DR483_1 (2.6±0.6 %/decade), DR370_1 (2.2±0.6 %/decade), and DR469 (2.1±0.7 %/decade). From these fading rates, a weighted average *g* value of 2.5±0.3 %/decade was calculated and used to correct the other samples. Table 3 lists both uncorrected and fading-corrected ages, while in the text the fading-corrected values are given.

These fading rates are comparable to those obtained on glaciofluvial deposits derived from crystalline basement of the swiss alps (e.g., Gaar et al. 2014; Lowick et al. 2012) or are even lower than from sediments derived from recycled Precambrian terranes of Northern America (Huntley and Lamothe 2001). They are also far lower than the observed signal loss in Sanidine by Wintle (1973), supporting the premise that the K-feldspar grains sampled from the phreatomagmatic deposits are of primarily plutonic or metamorphic origin and that contamination by volcanic K-feldspar is minor in the analyzed separates.

Samples, luminescence age results, and discussion

Lake Andraikiba area

A total of seven samples were taken for luminescence dating from six stratigraphic sections within a 2-km radius from the Lake Andraikiba crater (Fig. 4). Three samples were obtained from the upper phreatomagmatic unit, associated with the main Lake Andraikiba maar eruption, and four samples from the lower phreatomagmatic unit.

The three IRSL ages of 58±4 ka (sample DR361_3), 47±7 ka (sample DR471_2), and 56±7 ka (sample DR469) from the upper unit (Fig. 4; Table 3) give an average age of 54±5 ka (arithmetic mean, 1 SD). Based on the good agreement of the individual ages, which overlap within error, and the stratigraphic deliberations given in the above paragraphs, this average age is taken as the eruption age of the Lake Andraikiba maar.

For the lower phreatomagmatic unit in the Lake Andraikiba area, IRSL ages for three out of four samples yield IRSL ages of 109±15 ka (sample DR488), 107±12 ka (sample DR361_1), and 90±11 ka (sample DR361_2) (Fig. 4; Table 3), with a mean of 102±9 ka. The significance of an older age at 157±25 ka (sample DR471_1) in section 471 remains unclear. While the sampled deposit giving this older age seems to lie in the same stratigraphic position, it has a significantly different U/Th ratio (Table 2). This observation and the fact that there is no compelling reason to discard this age based on analytical problems suggests the possible presence of an even older phreatomagmatic explosion deposit outcropping at this location.

The geographical source for the (average age) 102±9 ka phreatomagmatic eruption unit is not clear. A possible candidate is the Amboniloha volcanic complex, approximately 4 km to the northeast (Fig. 3). There, an explosion breccia crops out along the flank of one of the older cones. It contains a high fraction of Precambrian basement blocks up to several decimeters and of similarly sized older basalt blocks, which suggests a proximal deposit. This breccia is directly overlain by unsorted deposits of black tephra containing juvenile volcanic bombs and blocks of decimeter scale, with some of the blocks containing xenoliths of crystalline material identical to the underlying explosion breccia. It is assumed that the tephra originated from the nearby Amboniloha cones. This is corroborated by the fact that material from the explosion breccia is not found on the surface of a small late-stage basanitic flow from this vent. Mottet (1980b) stratigraphically correlates the youngest Amboniloha tephra with similar pyroclastic material "found in some outcrops on the eastern (but not the western) flank of the Lake Andraikiba maar crater, where they are covered by the main Andraikiba eruption layer." A similar tephra sequence between the lower phreatomagmatic deposit overlying the weathered old basalt flow and the overlying Andraikiba phreatomagmatic eruption deposit is also found in an isolated outcrop along the western lake shore (coordinates, 46° 57.836′ E, 19° 52.329′ S), but has not been observed in other outcrops. These observations suggest the following relative chronological sequence: old laterized basalt; presumed Amboniloha phreatomagmatic eruption at 102±9 ka (lower phreatomagmatic unit at Lake Andraikiba); Amboniloha tephra (presumably only preserved as relicts at Andraikiba); main Andraikiba phreatomagmatic eruption at 54±5 ka and subsequently change to more strombolian activity at Andraikiba.

In summary, the obtained IRSL ages from the Lake Andraikiba area are in stratigraphic order and are consistent for individual stratigraphic units in different sections. The observed pedogenesis in the lower unit accords with the observed hiatus in the numerical ages between the lower and upper phreatomagmatic units.

Table 3 Equivalent doses (D_e) and luminescence ages

Area	Sample	$D_{e\ 60}$ (Gy)	n_{60}	$D_{e\ 10}$ (Gy)	n_{10}	RSD[a]	Age_{60} (ka)	Age_{10} (ka)	Age_{avg} (ka)	Corr. Age_{avg} (ka)
Lake Andraikiba Lower Upper	DR361_3	204±6	22	221±13	11	16 %	45±3	49±4	47±3	58±4
	DR471_2	175±16	8	140±6	34	27 %	47±5	38±3	38±3[b]	47±7
	DR469	174±7	13	181±8	12	14 %	46±4	48±4	47±3	56±7[d]
	DR488	249±7	19	258±11	24	17 %	81±6	84±7	82±5	109±15[d]
	DR361_2	195±7	27	196±15	10	19 %	72±5	73±7	72±4	90±11
	DR361_1	210±8	28	n.a.	n.a.	19 %	81±6	n.a.	81±6[a]	107±12
	DR471_1	243±9	25	n.a.	n.a.	18 %	125±14	n.a.	125±14[a, c]	157±25
Ampasami-haiky	DR340_1	99±11	3	71±6	12	27 %	55±7	40±4	40±4[b]	49±9
	DR340_2	116±4	26	112±4	20	17 %	56±4	54±4	55±3	68±7
Fizinana	DR370_2	159±6	31	n.a.	n.a.	21 %	65±4	n.a.	65±4[a]	81±9
	DR370_1	165±7	11	168±10	12	18 %	53±4	54±4	54±3	65±8[d]
Lake Tritrivakely	DR483_2	49±3	3	41±2	12	15 %	19±2	16±1	16±1[b]	19±2
	DR483_1	71±3	18	64±1	24	12 %	27±2	24±1	26±1	32±3[d]

Values with indices 60 or 10 indicate measurements made with 60 or 10 s preheat, respectively; *n* is the number of aliquots measured. Age_{avg} is the average between Age_{60} and Age_{10} using error propagation, *RSD* is the relative standard deviation of the combined data sets. Corrected ages are based on Age_{avg}

[a] The only available age is given, not an average

[b] The statistically arguable age (due to low n) is not considered in the average

[c] For a discussion of this age, see text

[d] Age correction using actual *g* value determined for this sample (see text)

Lake Tritrivakely

At Lake Tritrivakely, both phreatomagmatic units were sampled in an outcrop on the southern rim of the crater. IRSL ages are 32±3 ka (sample DR483_1) for the lower and 19±2 ka (sample DR483_2) for the upper sampled unit (Table 3). As no clearly identifiable remains of these deposits have been found on the steeper parts of the volcanic rampart, which is most likely a consequence of the high erosion potential of these only lightly consolidated deposits, and assuming that the deposits blanketed the entire crater, sandy layers comprised of the same material should also be evident in the crater infill sediments, both from the initial deposition as well as due to later reworking of such material from the rampart.

A 40-m sedimentary sequence was recovered through piston coring from Lake Tritrivakely (Gasse et al. 1994; Gasse and Van Campo 1998, 2001). Fourteen AMS ^{14}C dates on Cyperaceae debris and charcoal constrain the chronology of the upper 13 m of the sequence to between 0 and 36.2 ka BP (Gasse et al. 1994). Gasse and Van Campo (1998) converted the ^{14}C ages to calendar years (cal ka BP) and correlated the depth- and time-scale assuming constant sedimentation rate between successive calibrated ages. The stratigraphic logs of Gasse and Van Campo (1998) show two prominent sandy sections in the upper 13 m of the core. From 1,250 to 1,143 cm (40–38 cal ka BP), fine sandy material and oxidized clay alternate with organic-rich clay layers and from 452 to 402 cm (22–17 cal ka BP) fine sand lenses are interbedded within oxidized clay (Gasse and Van Campo 1998). An airfall tephra layer at 1,175–1,170 cm (Gasse and Van Campo 1998) indicates a volcanic event in the region, even though it need not be directly related to the eruption activity which caused the two observed phreatomagmatic deposits found at Lake Tritrivakely. Comparing the ^{14}C ages with the luminescence data, we note that the 32±3 ka IRSL age of the lower phreatomagmatic eruption deposit lies close to the inferred age (40–38 cal ka BP) of the sandy layers at c. 12-m depth, whereas the IRSL age of 19±2 ka for the upper deposit corresponds well with the occurrence of fine sand lenses in the drill core between c. 4.5 and 4-m depth, whose inferred age lies between 22 and 17 cal ka BP.

Fizinana and Ampasamihaiky areas

Samples were obtained from the lower phreatomagmatic deposit directly overlying the old laterite and from the uppermost such deposit both in the Fizinana (section 370) and Ampasamihaiky area (section 340) (Figs. 8 and 11). IRSL ages for the lower deposit are almost identical: 65±8 ka (sample DR370_1) for the Fizinana area and 68±7 ka (sample DR340_2) for the Ampasamihaiky area (Fig. 11; Table 3). The corresponding ages in combination with the similar

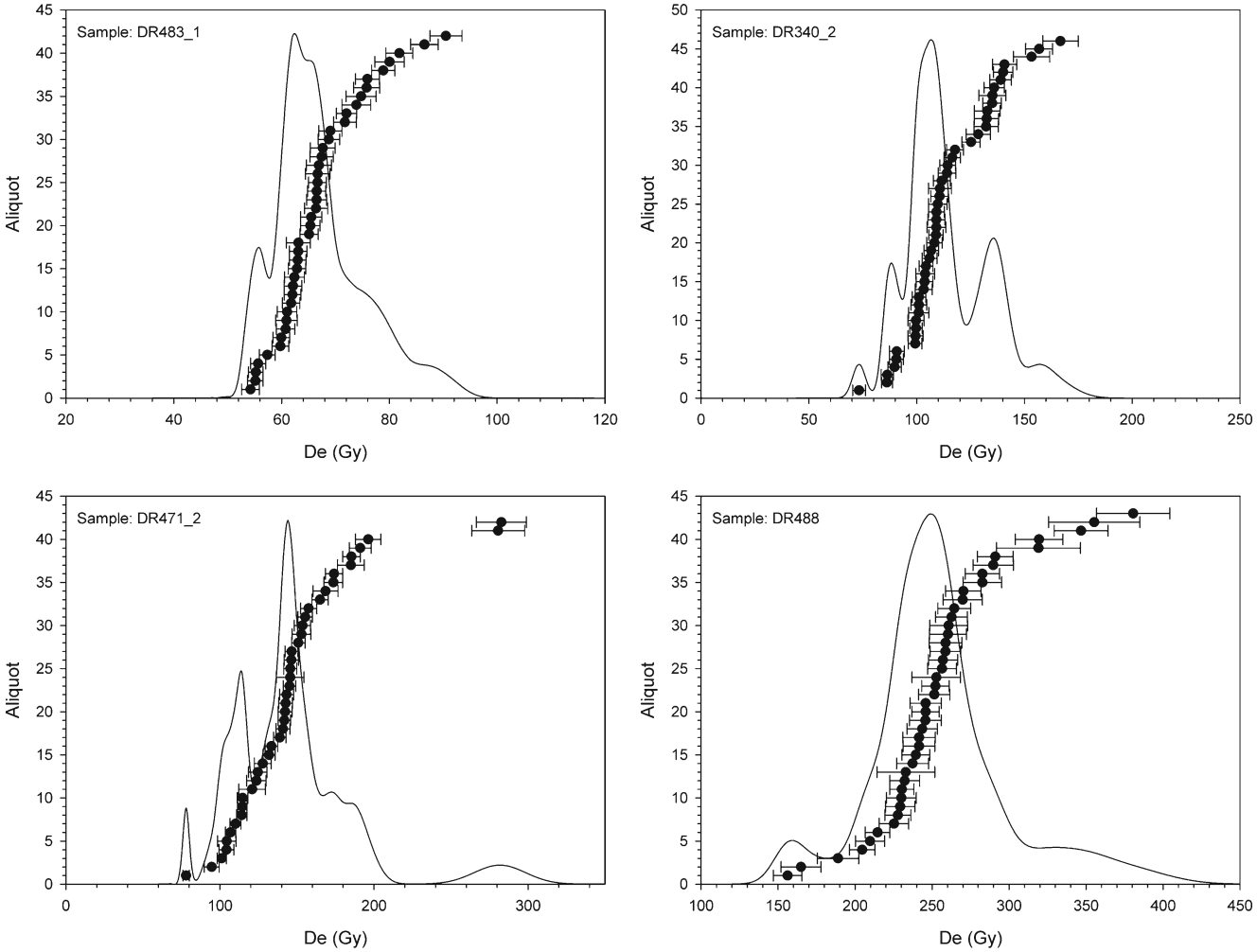

Fig. 16 Dose distribution plot of four representative IRSL samples. The Gaussian-like spread of D_e values together with the relative standard deviations is interpreted as indicators for complete resetting of the IRSL signal during the eruption

mineralogical composition and the fact that this eruption deposit forms the lowermost unit directly on top of a massive older laterite strongly suggests that these units can be stratigraphically correlated.

The sample from the upper phreatomagmatic eruption unit in the Ampasamihaiky area yields an age of 49±9 ka (sample DR340_1), which is in stratigraphic order and accommodates for the underlying palaeosoil (Fig. 11; Table 3). While this latter age is similar to the ages from the main Andraikiba eruption deposits, it would probably be presumptuous to make a correlation based on this single sample. In the Fizinana section, the luminescence age for the upper sample is 81± 9 ka (sample DR370_2). This is the only age that appears, at a first glance, not being in stratigraphic order compared to the age of 65±8 ka (sample DR370_1) obtained from the stratigraphically underlying phreatomagmatic eruption deposit from the same section (Figs. 11 and 14). However, both ages agree within uncertainties (Table 3).

Reliability of IRSL ages

Since a novel dating approach has been used in this study, it appears appropriate to discuss whether or not the reported IRSL ages are reliable. Firstly, the observed IRSL signals are far from saturation, indicating that resetting must have occurred during the eruption. The spread of repeated D_e measurements is Gaussian-like (Fig. 16), with relative standard deviations between 12 and 27 %, indicative for homogenous, thus likely complete resetting of the signal (cf. Preusser et al. 2007). Secondly, the IRSL ages are consistent with the observed relative stratigraphy, which would be unlikely for intercalated deposits of different eruptions in the case of incomplete resetting. Thirdly, IRSL ages of the two phreatomagmatic eruption deposits on the inner rim of Lake Tritrivakely fit well with the timing of deposition of the sandy sections in the drill core. These points, together with the demonstrated cardinal applicability of the method for dating

such deposits (Preusser et al. 2011), provide supporting arguments for the reliability of the presented IRSL ages.

Conclusions

This study provides the first direct numerical ages of phreatomagmatic eruption deposits in Madagascar and demonstrates the applicability of IRSL dating in this context. We obtained 13 IRSL K-feldspar ages from samples in the Vakinankaratra volcanic field. All ages are in stratigraphic order and ages obtained from units that can be correlated stratigraphically correspond closely. Our results indicate Late Pleistocene phreatomagmatic eruption activity in the Antsirabe-Betafo region. The age of the Lake Andraikiba maar formation is dated to 54±5 ka, and an older phreatomagmatic eruption deposit from the same region was dated to 102±9 ka. In the area of Betafo, a phreatomagmatic explosion unit underlying volcanic deposits of scoria cones was dated at approximately 68 ka. This age provides an upper age limit to the subsequently developed Iavoko, Antsifotra and Fizinana scoria cones, and their associated lava flows. At Lake Tritrivakely, two allochthonous phreatomagmatic deposits yielded ages of 32±3 and 19±2 ka, respectively.

Acknowledgements Financial support for this project was provided by the Swiss National Foundation (SNF), Project numbers 200020-105453/1, 200020-118023/1, and 206021–117374, and the Berne University Research Foundation. Sönke Szidat is thanked for high-resolution gamma spectrometry measurements, Marco Herwegh for introducing DR to the SEM, and Jörg Giese, Sally Lowick, Inga Schindelwig, Damian Steffen, Michèle Suchy, and Mareike Trauerstein for helpful discussions and comments. We acknowledge helpful comments from two anonymous reviewers and thank executive editor James D. L. White for additional critical comments which helped to improve the manuscript.

References

Aitken MJ (1985) Thermoluminescence Dating. Academic, London

Bardintzeff JM, Liégois JP, Bonin B, Bellon H, Rasamimanana G (2010) Madagascar volcanic provinces linked to the Gondwana break-up: geochemical and isotopic evidences for contrasting mantle sources. Gondwana Res 18:295–314

Bassinet C, Mercier N, Miallier D, Pilleyre T, Sanzelle S, Valladas H (2006) Thermoluminescence of heated quartz grains: intercomparisons between SAR and multiple-aliquot additive dose techniques. Radiat Meas 41:803–808

Berger A, Gnos E, Rakotondrazafy M, Rufer D, Schreurs G (2008) Geological Map west of Antsirabe (1: 40,000)

Bertil D, Regnoult JM (1998) Seismotectonics of Madagascar. Tectonophysics 294:57–74

Besairie H (1964) Carte Géologique de Madagascar. 1:1000 000. Service Géologique de Madagascar, Antananarivo

Besairie H, Besairie H (1969) Carte Géologique. Feuille 5. 1:500 000. Service Géologique de Madagascar, Antananarivo

Bonde A, Murray A, Friedrich WL (2001) Santorini: luminescence dating of a volcanic province using quartz. Quat Sci Rev 20:789–793

Büttner R, Zimanowski B (1998) Physics of thermohydraulic explosions. Phys Rev E 57:5726–5729

Duller GAT (1992) Luminescence chronology of raised marine terraces, south-west North Island, New Zealand. Dissertation, University Of Wales, Aberystwyth, p 147

Fattahi M, Stokes S (2000) Extending the time range of luminescence dating using red TL (RTL) from volcanic quartz. Radiat Meas 32: 479–485

Fattahi M, Stokes S (2003) Dating volcanic and related sediments by luminescence methods: a review. Earth Sci Rev 62:229–264

Faure G (1986) Principles of isotope geology, 2nd edn. John Wiley & Sons, New York

Gaar D, Lowick SE, Preusser F (2014) Performance of different luminescence approaches for the dating of known-age glaciofluvial deposits from northern Switzerland. Geochronometria 41:65–80

Ganzawa Y, Furukawa H, Hashimoto T, Sanzelle S, Miallier D, Pilleyre T (2005) Single grains dating of volcanic quartz from pyroclastic flows using Red TL. Radiat Meas 39:479–487

Gasse F, Van Campo E (1998) A 40,000-yr pollen and diatom record from Lake Tritrivakely, Madagascar, in the southern tropics. Quat Res 49: 299–311

Gasse F, Van Campo E (2001) Late Quaternary environmental changes from a pollen and diatom record in the southern tropics (Lake Tritrivakely, Madagascar). Palaeogeogr Palaeoclimatol Palaeoecol 167:287–308

Gasse F, Cortijo E, Disnar JR, Ferry L, Gibert E, Kissel C, Laggoundefarge F, Lallierverges E, Miskovsky JC, Ratsimbazafy B, Ranaivo F, Robison L, Tucholka P, Saos JL, Siffedine A, Taieb M, Van Campo E, Williamson D (1994) A 36-ka environmental record in the southern tropics—Lake Tritrivakely (Madagascar). Comptes Rendus de L'academie des Sciences—Serie II 318:1513–1519

Grimison NL, Chen WP (1988) Earthquakes in the Davie Ridge-Madagascar Region and the Southern Nubian-Somalian Plate Boundary. J Geophys Res—Solid 93:10439–10450

Huntley DJ, Baril MR (1997) The K content of the K-feldspars being measured in optical dating or in thermoluminescence dating. Ancient TL 15:11–14

Huntley DJ, Lamothe M (2001) Ubiquity of anomalous fading in K-feldspars and the measurement and correction for it in optical dating. Can J Earth Sci 38:1093–1106

Israelson OW, West FL (1922) Water holding capacity of irrigated soils. Utah State Agric Exp Stat Bull 183:1–24

Kars RH, Wallinga J, Cohen KM (2008) A new approach towards anomalous fading correction for feldspar IRSL dating—tests on samples in field saturation. Radiat Meas 43:786–790

Kulig G (2005) Erstellung einer Auswertesoftware zur Alterbestimmung mittels Lumineszensverfahren unter spezieller Berücksichtigung des Einflusses radioaktiver Ungleichgewichte in der ^{238}U-Zerfallsreihe. Unpublished Bsc Dissertation, Technical University Bergakademie Freiberg

Kusky TM, Toraman E, Raharimahefa T (2007) The Great Rift Valley of Madagascar: an extension of the Africa-Somali diffusive plate boundary? Gondwana Res 11:577–579

Kusky TM, Toraman E, Raharimahefa T, Rasoazanamparany C (2010) Active tectonics of the Alaotra-Ankay graben system, Madagascar: possible extension of Somalian-African diffusive plate boundary? Gondwana Res 18:274–294

Lacroix A (1921–1923) La minéralogie de Madagascar. Paris

Lamothe M, Auclair M, Hamzaoui C, Huot S (2003) Towards a prediction of long-term anomalous fading of feldspar IRSL. Radiat Meas 37:493–498

Laville E, Piqué A, Plaziat JC, Gioan P, Rakotomalala R, Ravololonirina Y, Tidahy E (1998) Le fosse meridien d'Ankay-Alaotra, témoin d'une extension crustale récente et actuelle à Madagascar. Bull Soc géol France 169:775–788

Lowick SE, Trauerstein M, Preusser F (2012) Testing the application of post IR-IRSL dating to fine grain waterlain sediments. Quat Geochronol 8:33–40

Mejdahl V (1985) Thermoluminescence dating of partially bleached sediments. Nucl Tracks Radiat Meas 10:711–715

Mottet G. (1980a) L'Ankaratra et ses bordures (Madagascar): Recherches de Géomorphologie volcanique—Tome I, Le massif de l'Ankaratra. Dissertation, Université de Lyon

Mottet G. (1980b): L'Ankaratra et ses bordures (Madagascar): Recherches de Géomorphologie volcanique. - Tome II, Les bordures et le volcanisme Quaternaire: Le volcanisme du massif des Vavavato, Le Vakinankaratra, Le Massif de l'Itasy. Dissertation, Université De Lyon

Mougenot D, Recq M, Virlogeux P, Lepvrier C (1986) Seaward extension of the East African Rift. Nature 321:599–603

Ollier CD (1974) Phreatic eruptions and maars. In: Civetta L et al (eds) Physical Volcanology. Elsevier, New York

Petit M (1998) Présentation physique de la grande île Madagascar. FTM—Institut Géographique Et Hydrographique National, Antananarivo

Piqué A, Laville E, Chotin P, Chorowicz J, Rakotondraompiana S, Thouin C (1999) Neogene and present extension in Madagascar: structural and geophysical data. J Afr Earth Sci 28:975–983

Preusser F (1999) Lumineszenzdatierungen fluviatiler Sedimente - Fallbeispiele aus der Schweiz und Norddeutschland. Kölner Forum für Geol und Paläontol 3:63

Preusser F, Blei A, Graf HR, Schlüchter C (2007) Luminescence dating of Würmian (Weichselian) proglacial sediments from Switzerland: methodological aspects and stratigraphical conclusions. Boreas 36: 130–142

Preusser F, Degering D, Fuchs M, Hilgers A, Kadereit A, Klasen N, Krbetschek M, Richter D, Spencer JQG (2008) Luminescence dating: basics, methods and applications. E&G Quat Sci J 57:95–149

Preusser F, Rufer D, Schreurs G (2011) Direct dating of Quaternary phreatic maar eruptions by luminescence methods. Geology 39: 1135–1138

Randriantsoa MM (2001) Rôle de la matière organique dans la fertilité phosphorique d'un sol ferrallitique des Hautes Terres Malgaches. DEA de l'institut national polytechnique de Lorraine. Cirad-Tafa, 26p

Rasamimanana G, Bardintzeff JM, Rasendrasoa J, Bellon H, Thouin C, Gioan P, Piqué A (1998) Les episodes magmatiques du Sud-Ouest de Madagascar (basin de Morondava), marqueurs des phénomènes de rifting crétacé et néogène. CR Acad Sci Paris 326:685–691

Rufer D, Gnos E, Mettier F, Preusser F, Schreurs G (2012) Proposing new approaches for dating young volcanic eruptions by luminescence methods. Geochronometria 39:48–56

Schmincke HU (1977) Phreatomagmatische Phasen in Quartären Vulkanen der Osteifel. Geol Jahrb A39:3–45

Sheridan MF, Wohletz KH (1981) Hydrovolcanic explosions: the systematics of water-pyroclast equilibration. Science 212:1387–1389

Sheridan MF, Wohletz KH (1983) Hydrovolcanism: basic considerations and review. J Volcanol Geotherm Res 17:1–29

Sibree RJ (1891) The volcanic lake of Tritriva, Central Madagascar. Proc Royal Geogr Soc Monthly Rec Geogr 13:477–483

Sifeddine A, Laggoundefarge F, Lallierverges E, Disnar JR, Williamson D, Gasse F, Gibert E (1995) La sedimentation organique lacustre en zone tropicale sud au cours des 36 000 dernières années (Lac Tritrivakely, Madagascar). CR Acad Sci Paris 321:385–391

Steffen D, Preusser F, Schlunegger F (2009) OSL quartz age underestimation due to unstable signal components. Quat Geochronol 4:353–362

Tsukamoto S, Murray AS, Huot S, Watanuki T, Denby PM, Bøtter-Jensen L (2007) Luminescence property of volcanic quartz and the use of red isothermal TL for dating tephras. Radiat Meas 42:190–197

Tucker RD, Moine B (2012) Discussion of: Petrogenesis and Nd-, Pb-, Sr-isotope geochemistry of the Cenozoic olivine melilites and olivine nephelinites ("Ankaratrites") in Madagascar. Lithos 140(141): 255–256

Wallinga J, Murray A, Wintle A (2000) The single-aliquot regenerative-dose (SAR) protocol applied to coarse-grain feldspar. Radiat Meas 32:529–533

Wallinga J, Bos AJJ, Dorenbos P, Murray AS, Schokker J (2007) A test case for anomalous fading correction in IRSL dating. Quat Geochron 2:216–221

White JDL (1996) Impure coolants and interaction dynamics of phreatomagmatic eruptions. J Volcanol Geotherm Res 74:155–170

White JDL, Ross PS (2011) Maar-diatreme volcanoes: a review. J Volcanol Geotherm Res 201:1–29

Williamson D, Jelinowska A, Kissel C, Tucholka P, Gibert E, Gasse F, Massault M, Taieb M, Van Campo E, Wieckowski K (1998) Mineral-magnetic proxies of erosion/oxidation cycles in tropical maar-lake sediments (Lake Tritrivakely, Madagascar): paleoenvironmental implications. Earth Planet Sci Lett 155:205–219

Wintle AG (1973) Anomalous fading of thermoluminescence in mineral samples. Nature 245:143–144

Wohletz KH, Heiken G (1992) Volcanology and Geothermal Energy. University of California Press, Berkeley

Wohletz KH, Sheridan MF (1983) Hydrovolcanic explosions II: evolution of basaltic tuff rings and tuff cones. Am J Sci 283:385–413

Woolley AR (2001) Alkaline rocks and carbonatites of the world, Part 3: Africa. The Geological Society Publishing House, Bath, UK

Zebrowski C, Ratsimbazafy C (1979) Carte pédologique de Madagascar à 1:100,000—Notice Explicative No. 83